Catalytic dehydrocoupling of PhSiH$_3$ with bimetallic Ti and Zr complexes

Jean L. Huhmann, Joyce Y. Corey *, Nigam P. Rath

University of Missouri-St. Louis, St. Louis, MO 63121, USA

Abstract

Bimetallic titanium and zirconium complexes with bridges (X) between Cp ligands were compared to Cp$_2$MCl$_2$ as catalysts in the presence of ^{n}BuLi for the dehydrocoupling of PhSiH$_3$ to polyphenylsilane. The monobridged bimetallic complexes developed were of the composition [μ-X(C$_5$H$_4$)$_2$][CpMCl]$_2$ with X = Me$_2$Si (M = Ti, Zr), Me$_2$SiCH$_2$SiMe$_2$ (M = Ti) and Me$_2$SiCH$_2$CH$_2$SiMe$_2$ (M = Ti, Zr). The dibridged bimetallic complexes examined were of the type [μ,μ-(Me$_2$Si)$_2$(C$_5$H$_3$)$_2$][Cp$'$:'ZCl$_2$]$_2$ (Cp$'$ = Cp, *trans* isomer, Cp$'$ = Cp*, *trans* and *cis* isomers). There was not a significant difference in the molecular weight of the polysilane produced from Cp$_2$TiCl$_2$ and the bimetallic titanium complexes after 48 h of reaction. However, the polysilane which was generated from the bimetallic complex [μ-(Me$_2$Si)(C$_5$H$_4$)][CpZrCl$_2$]$_2$ was approximately twice the molecular weight compared to that obtained from Cp$_2$ZrCl$_2$. The structure of the bimetallic complex [μ-(Me$_2$SiCH$_2$CH$_2$SiMe$_2$)(C$_5$H$_4$)$_2$][CpZrCl$_2$]$_2$ was determined by X-ray diffraction (monoclinic, $P2_1/n$, $a = 8.7297(3)$ Å, $b = 6.7890(2)$ Å, $c = 24.9343(7)$ Å, $\beta = 93.7850(10)°$, $Z = 2$).

Keywords: Titanium; Zirconium; Silicon; Dehydrocoupling; Polysilanes; Polymerization

1. Introduction

Polysilanes are a relatively new class of polymer in which the backbone consists entirely of silicon atoms. An important characteristic of polysilanes is the strong σ-delocalization of electrons along the silicon backbone, leading to interesting electronic properties which are not available from related carbon-based polymers [1,2]. Polysilanes have been used as precursors to silicon carbide and have potential uses in microlithography and non-linear optics. The method generally employed for the preparation of polysilanes is the coupling of chlorosilanes with alkali metals (Wurtz-type coupling). However, this method is limited in that the yields are generally low, large amounts of salt waste are produced and the reaction can be difficult to control. A major drawback of the Wurtz-type coupling process is the inability to incorporate a range of functional groups on the silicon backbone, limiting the potential properties of the polymer [1,2].
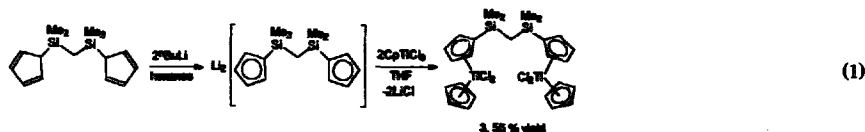
In recent years, much attention has been focused on the formation of polysilanes from the dehydrocoupling of hydrosilanes in the presence of a Group 4 metallocene catalyst [3–14]. The first effective silane dehydrocoupling catalyst was Cp$_2$MMe$_2$ (M = Ti, Zr, Cp = η^5-C$_5$H$_5$), which was reported in 1985 by Harrod and co-workers [3] to initiate the condensation of primary hydrosilanes to polysilanes [3]. Following this discovery, other Group 4 metallocene systems that are effective dehydrocoupling silane catalysts have been developed, including CpCp*MR$_1$R$_2$ (Cp* = η^5-C$_5$Me$_5$, M = Zr, Hf, R$_1$ = Si(SiMe$_3$)$_3$, SiH$_2$Ph; R$_2$ = SiMe$_3$, Me, Cl) by Tilley and co-workers [7–9], and Cp$_2$TiPh$_2$ by Nagai and co-workers [10]. We have reported the in situ generation of a silane dehydrocoupling catalyst derived from the combination of Cp$_2$MCl$_2$ (M = Ti, Zr, Hf) and ^{n}BuLi, as well as catalysts derived from *ansa* and substituted Group 4 metallocene dichlorides [11–14]. The currently accepted mechanism for Si–Si bond formation in the dehydrocoupling process with Group 4 metallocene-based catalysts involves a σ-bond metathesis step which was originally proposed by Tilley and co-workers [7–9]. We have suggested a pathway for the formation of polysilanes starting from Cp$_2$MCl$_2$ and

* Corresponding author.

2 equiv. of ^{n}BuLi, as shown in Scheme 1 for $R_1R_2SiH_2$ [11–14].

The silane used in the majority of these studies is $PhSiH_3$, which dehydrocouples to a mixture of linear $H(PhSiH)_xH$ and cyclic $(PhSiH)_x$ polyphenylsilane. The average molecular weight M_w values for the mixtures from the dehydrocoupling reactions of this silane generally fall in the range of 1000 to 4000, although Tilley and Imori have achieved polyphenylsilane with M_w values up to 12000 with the $CpCp*ZrR_1R_2$ catalyst precursor [9] and Dioumaev and Harrod have reported polyphenylsilane with an M_w of 14000 using $CpCp*ZrCl_2$ in the presence of ^{n}BuLi and $(C_6F_5)_3B$ [6]. Polyphenylsilane contains SiH and SiPh functional groups in the polymer backbone, both of which can be converted to a variety of other substituents by known methods [15]. Furthermore, polyphenylsilane of $M_w >$ 1000 is not accessible through Wurtz-type coupling of $PhSiHCl_2$ [1].

Bimetallic complexes have recently received attention in the literature due to their potential to exhibit cooperative reactivity which could be useful in catalysis (for several recent examples see Refs. [16–20]). The objective of the present study was to test bimetallic derivatives of the Group 4 metallocene system $Cp_2MCl_2/^{n}$BuLi as silane dehydrocoupling catalysts. The approach involved linking two Cp_2MCl_2 units with either one or two bridges X between Cp ligands, as illustrated in Fig. 1, and to compare the catalytic reactivity of these bimetallic complexes to that of the parent monometallic Cp_2MCl_2.

Rotation around X in monobridged bimetallic complexes may occur, thus the relative orientation of the two metal centers can vary in an uncontrollable manner. However, a dibridged bimetallic complex would offer a

Fig. 1.

less flexible system, with the two metal centers locked on either the same (*cis*) or opposite (*trans*) face of the $[\mu,\mu\text{-X}(C_5H_3)_2]$ moiety, as shown in Fig. 1. Cooperative reactivity in catalysis may be more likely to occur for the *cis* bimetallic complexes than for the corresponding *trans* derivatives since the catalytic sites in a *cis* complex will be held in close proximity. To study this, dibridged *cis* and *trans* bimetallic complexes were compared as catalysts in the presence of ^{n}BuLi for the dehydrocoupling of $PhSiH_3$.

Cooperative reactivity in a catalytic cycle may also be dependent on the relative distance between the two metal centers in the bimetallic complex. This distance will be influenced by the effective length and flexibility of the bridge X. If the length of X is too great, it may not be possible for the two metal centers to interact cooperatively, however if the length of X is too short, the metal centers may be too sterically crowded to interact. In an attempt to study this balance, a series of monobridged bimetallic with an increasing number of atoms in the bridge X were compared as dehydrocoupling catalysts in the presence of ^{n}BuLi for $PhSiH_3$.

2. Results and discussion

2.1. Preparation of the Ti and Zr bimetallic complexes.

The general method employed in this study to prepare bimetallic complexes was the reaction of 2 equiv. of $CpMCl_2$ with a source of either $[\mu\text{-X}(C_5H_4)_2]^{2-}$ or $[\mu,\mu\text{-X}_2(C_5H_3)_2]^{2-}$. Only complexes with bridges (X) which contained silicon atoms bonded to the C_5H_4 or C_5H_3 units were prepared in this study due to the ease of formation of Si–Cp bonds from LiCp sources and chlorosilanes. The titanium complex $[\mu\text{-(Me}_2\text{Si)-}(C_5H_4)_2][CpTiCl_2]_2$ (1) was synthesized as described by Nifant'ev et al. from the reaction of $CpTiCl_3$ with $[Me_2Sn][\mu\text{-(Me}_2\text{Si)(C}_5H_4)_2]$ in THF [18]. The corre-

Scheme 1. Proposed mechanism for the dehydrocoupling of $R_1R_2SiH_2$.

Fig. 2.

sponding zirconium analog $[\mu\text{-}(Me_2Si)(C_5H_4)_2]$-$[CpZrCl_2]_2$ (2) was prepared from the salt elimination reaction of $Li_2[\mu\text{-}(Me_2Si)(C_5H_4)_2]$ and $CpZrCl_3(THF)_2$ in toluene, as previously reported by Reddy and Petersen [16]. Complexes 1 and 2 are shown in Fig. 2.

The reaction of the known compound $[\mu\text{-}(Me_2SiCH_2SiMe_2)(C_5H_5)_2]$ [21] with 2 equiv. of ^nBuLi in hexanes produced $Li_2[\mu\text{-}(Me_2SiCH_2SiMe_2)\text{-}(C_5H_4)_2]$, which was isolated as a white powder. Subsequent reaction of this dilithio salt with 2 equiv. of $CpTiCl_3$ in THF provided the new monobridged bimetallic complex $[\mu\text{-}(Me_2SiCH_2SiMe_2)(C_5H_4)_2]$-

$[CpTiCl_2]_2$ (3), as shown in Eq. (1). Complex 3 was obtained as orange microcrystals from the THF reaction mixture, and was purified by Soxhlet extraction with CH_2Cl_2 and isolated as the CH_2Cl_2 solvate (0.25 equiv) in a 55% yield. The presence of the 0.25 equiv CH_2Cl_2 was demonstrated in the ^1H NMR spectrum and in the elemental analysis results. Complex 3 was moderately soluble in CH_2Cl_2 and THF, and slightly soluble in aromatic hydrocarbons. The complex was air-stable at room temperature when isolated in the solid state, but sensitive to hydrolysis in THF and CH_2Cl_2 solutions. The zirconium analog of 3 was not prepared in this study.

$$(1)$$

Similarly, $Li_2[\mu\text{-}(Me_2SiCH_2CH_2SiMe_2)(C_5H_4)_2]$ was prepared from the known compound $[\mu\text{-}(Me_2SiCH_2CH_2SiMe_2)(C_5H_5)_2]$ [22] and ^nBuLi in hexanes. The dilithio salt was subsequently allowed to react with either $CpTiCl_3$ in THF solution to provide $[\mu\text{-}(Me_2SiCH_2CH_2SiMe_2)(C_5H_4)_2][CpTiCl_2]_2$ (4), or with $CpZrCl_3(THF)_2$ in a mixture of THF and hexanes to produce $[\mu\text{-}(Me_2SiCH_2CH_2SiMe_2)(C_5H_4)_2]$-$[CpZrCl_2]_2$ (5), as shown in Eq. (2). The titanium complex 4 exhibited similar solubility characteristics as

3, and was isolated as air-stable orange microcrystals from Soxhlet extraction with CH_2Cl_2 in a 50% yield, and was found to be a solvate which contained 0.25 equiv. of CH_2Cl_2. The zirconium complex 5 was obtained as white crystals in a 48% yield from a CH_2Cl_2–hexanes solution (the preparation of 5 was recently reported by a similar route [23]). Complex 5 was soluble in CH_2Cl_2, THF and toluene, and was air-stable at room temperature but sensitive to hydrolysis in solution.

$$(2)$$
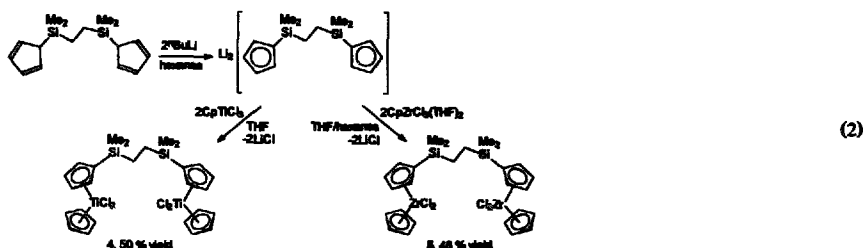
The NMR data obtained for the new complexes 3, 4 and 5 are very similar to that previously reported for 1 and 2 [16,18]. The ^1H NMR spectra for 3–5 showed one MeSi singlet, one CH_2 singlet, a singlet due to Cp (C_5H_5), and two pseudo triplets corresponding to the A_2B_2 pattern for the bridged C_5H_4 groups. The ^{13}C NMR spectra exhibited the expected number of signals,

and the ^{29}Si NMR spectra for each complex showed one silicon environment. Satisfactory elemental analyses were obtained for the CH_2Cl_2 solvates of 3 and 4, and for the complex 5. Complexes 1–5 represent a series of monobridged bimetallic complexes with one, three and four atoms in the bridging unit X. The corresponding titanium and zirconium complexes with a two atom
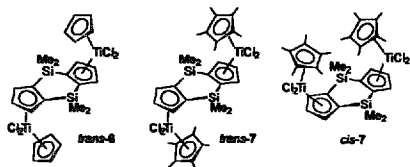
Fig. 3.

bridge ($X = Me_2SiSiMe_2$) were not used in this study owing to the possibility of Si–Si bond cleavage under dehydrocoupling conditions, although the complexes could be accessible from the known $Li_2[\mu\text{-}(Me_2SiSiMe_2)(C_5H_4)_2]$ and $CpMCl_3$ [24].

The dibridged bimetallic complexes utilized in this study were the titanium derivatives with two Me_2Si bridges shown in Fig. 3, the preparation and characterization of which have been previously described [25]. The *trans* isomer of $[\mu,\mu\text{-}(Me_2Si)_2(C_5H_3)_2][CpTiCl_2]_2$ (6) was prepared from the reaction of $Li_2[\mu,\mu\text{-}(Me_2Si)_2(C_5H_3)_2]$ with 2 equiv. of $CpTiCl_3$ in THF solution. The *trans* and *cis* isomers of $[\mu,\mu\text{-}(Me_2Si)_2(C_5H_3)_2][Cp*TiCl_2]_2$ (7) were obtained as a mixture from the reaction of $Li_2[\mu,\mu\text{-}(Me_2Si)_2(C_5H_3)_2]$ with $Cp*TiCl_3$, and separated by fractional crystallization [25].

2.2. X-ray crystal structure of $[\mu\text{-}(Me_2Si\text{-}CH_2CH_2SiMe_2)(C_5H_4)_2][CpZrCl_2]_2$ (5)

Recrystallization of 5 in a CH_2Cl_2 solution at room temperature provided colorless prisms which were suitable for X-ray diffraction studies. Experimental details of the structure determination are provided in Table 1, and the atomic coordinates for the non-hydrogen atoms are in Table 2. Table 3 lists selected geometric parameters. A projection view of 5 with the thermal ellipsoids drawn at 50% probability and showing the atomic labeling scheme (hydrogen atoms not shown) is presented in Fig. 4.

The structure of 5 has a center of symmetry, thus only half of the molecule is unique. The Cp carbons were disordered, and were refined as [C(6)–C(10)] (53% occupancy) and [C(6′)–C(10′)] (47% occupancy). There are no unusual bond lengths or angles in the structure. The two $ZrCl_2$ groups in the molecule are oriented in opposite directions, as are the two Me_2Si groups. Furthermore, the zirconium atoms are positioned on opposite sides of the plane defined by the two silicon atoms, Si(1) and Si(1A), and the two bridgehead carbon atoms of two C_5H_4 groups, C(1) and C(1A). The non-bonded distance between the two zirconium atoms is approximately 11.3 Å, and the non-bonded distance between the two silicon atoms is approximately 4.6 Å.

The structure of 5 may be compared to the known structures of the bimetallic compounds $[\mu\text{-}(Me_2Si)(C_5H_4)][Cp*MCl_2]_2$, where M is Ti [26] and Zr [16]. Neither of these two previously reported structures with a one-atom bridge ($X = Me_2Si$) contain a center of symmetry. Due to the bulkiness of the Cp* groups, the M atoms are on the same side of the plane

Table 1
Crystallographic data for $[\mu\text{-}(Me_2SiCH_2CH_2SiMe_2)(C_5H_4)_2][CpZrCl_2]_2$.

Crystal system	Monoclinic
Space group	$P2_1/n$
a (Å)	8.7297(3)
b (Å)	6.7890(2)
c (Å)	24.9343(7)
β (deg)	93.7850(10)
V (Å^3)	1474.53(8)
Z	2
D_c (g cm^{-3})	1.637
T (K)	193(2)
Radiation	Mo Kα ($\lambda = 0.71073$ Å)
μ (mm^{-1})	1.165
2θ range (deg)	3.28 to 52.00
Reflections collected	9275
Independent reflections	2898 ($R_{int} = 0.0881$)
Data/restraints/parameters	2854/0/171
Final R indices [$I > 2\sigma I$]	$R1 = 0.0541$, $wR2 = 0.1406$
R indices (all data)	$R1 = 0.0861$, $wR2 = 0.1743$
Goodness of fit (F^2)	1.107

Table 2
Atomic coordinates ($\times 10^4$) and equivalent isotropic displacement parameters (Å$^2 \times 10^3$) for $[\mu\text{-}(Me_2SiCH_2CH_2SiMe_2)\text{-}(C_5H_4)_2][CpZrCl_2]_2$

	x	y	z	U_{eq} [a]
Zr(1)	5422(1)	4756(1)	1505(1)	20(1)
Cl(1)	6623(2)	2083(2)	2043(1)	32(1)
Cl(2)	4116(2)	2683(2)	821(1)	34(1)
Si(1)	8726(2)	2870(2)	541(1)	24(1)
C(1)	7733(6)	4823(9)	919(2)	23(1)
C(2)	8220(6)	5600(9)	1433(3)	26(3)
C(3)	7422(7)	7333(9)	1533(3)	30(2)
C(4)	6411(8)	7728(9)	1074(3)	35(2)
C(5)	6616(7)	6214(9)	699(3)	27(1)
C(6)	2668(25)	5218(44)	1696(12)	41(6)
C(7)	3405(32)	4361(29)	2152(11)	32(5)
C(8)	4469(37)	5519(68)	2429(15)	53(8)
C(9)	4408(25)	7362(21)	2089(11)	25(4)
C(10)	3297(26)	7067(47)	1643(8)	38(5)
C(6′)	2896(28)	4524(46)	1955(14)	41(6)
C(7′)	4028(42)	5116(71)	2331(12)	61(11)
C(8′)	4542(27)	6687(66)	2267(10)	53(8)
C(9′)	3804(28)	7561(21)	1804(11)	25(4)
C(10′)	2775(27)	6233(52)	1598(9)	38(5)
C(11)	9665(7)	1041(10)	1013(3)	34(2)
C(12)	7368(8)	1706(10)	27(3)	36(2)
C(13)	10272(7)	4175(9)	194(3)	28(1)

[a] U_{eq} is defined as one-third of the trace of the orthongonalized U_{ij} tensor.

Table 3
Selected geometric parameters for [μ-(Me$_2$SiCH$_2$CH$_2$SiMe$_2$)(C$_5$H$_4$)$_2$][CpZrCl$_2$]$_2$ [a]

Bond lengths (Å)		Non-bonded distances (Å) and angles (deg)	
Si(1)–C(11)	1.863(7)	Zr(1)–Cp(1)$_{cent}$	2.203
Si(1)–C(12)	1.864(7)	Zr(1)–Cp(2)$_{cent}$	2.189
Si(1)–C(13)	1.873(6)	Zr(1)–Zr(1A)	11.326
Si(1)–C(1)	1.873(6)	Si(1)–Si(1A)	4.625
C(13)–C(13A)	1.535(12)	Cp(1)$_{cent}$–Zr–Cp(2)$_{cent}$	129.5
Zr(1)–Cl(1)	2.450(2)	Cp(1)$_{cent}$–Zr–Cl(1)	107.0
Zr(1)–Cl(2)	2.437(2)	Cp(1)$_{cent}$–Zr–Cl(2)	108.0
		Cp(2)$_{cent}$–Zr–Cl(1)	104.3
Bond angles (deg)		Cp(2)$_{cent}$–Zr–Cl(2)	106.7
C(11)–Si(1)–C(12)	112.7(3)		
Cl(1)–Zr(1)–Cl(2)	96.85(6)		

[a] Cp(1)$_{cent}$ was calculated as the centroid derived from C(1), C(2), C(3), C(4) and C(5); Cp(2)$_{cent}$ was calculated as the centroid derived from C(6), C(7), C(8), C(9) and C(10).

defined by the Si atom and the bridgehead carbon atoms of the two C$_5$H$_4$ groups. The non-bonded M–M distances in these structures are 7.33 Å and 7.26 Å for M = Ti and Zr respectively. The difference between the M–M distance in 5, which has a four-atom bridge, and the average M–M distance for the two [μ-(Me$_2$Si)(C$_5$H$_4$)$_2$][Cp*MCl$_2$]$_2$ complexes, each of which has a one-atom bridge, is approximately 4.0 Å.

2.3. Dehydrocoupling reactions of PhSiH$_3$

Following the sequence outlined in Scheme 1, bimetallic complexes with bridges contained in the Cp ligands should react with [n]BuLi and R$_1$R$_2$SiH$_2$ to form R$_1$R$_2$SiHBu and the proposed active bimetallic catalyst [μ-X(Cp$_2$M)$_2$], as shown in Scheme 2. The insertion of each metal center into an Si–H bond could then provide the bimetallic silyl-hydride complex. At this point, either a cooperative or a non-cooperative pathway could be followed. In a non-cooperative mechanism, each metal center could undergo σ-bond metathesis steps to form Si–Si bonds, analogous to the mechanism for monometallic catalysts shown in Scheme 1. However, if the two metal centers in the bimetallic catalyst react in a cooperative manner, the mechanism may be quite different. It is possible that Si–Si bond formation could

still occur through a four-centered σ-bond metathesis step, but could now involve the Si–M bond of one metal center and the Si–H bond of the second metal center, as shown in Scheme 2. If this were the case, one might expect to obtain a different distribution of polysilane products from the dehydrocoupling of PhSiH$_3$ with monometallic and bimetallic complexes, or different rates of formation of the polysilane products.

Although many studies have focused on the synthesis and characterization of bimetallic Group 4 complexes which could have potential uses in catalysis [16–20], few reports have actually examined the effects of using bimetallic complexes in a catalytic process. One such example is a bimetallic zirconium system, [μ-(^{n}C$_6$H$_4$)(C$_5$H$_2$Me$_2$)$_2$][CpZrCl$_2$]$_2$, which was used in the presence of MAO to catalyze the polymerization of propene [19]. In this system, an increase in productivity was observed using the bimetallic catalyst compared to a monometallic analog, although slightly lower molecular weight polypropylene was produced. In another report, a dibridged bimetallic complex similar to that shown in Eq. (2), trans-[μ,μ-(Me$_2$Si)$_2$(C$_5$H$_3$)$_2$]-[(C$_5$H$_4$(SiMe$_3$))$_2$TiCl$_2$]$_2$, was used in the presence of MAO to polymerize ethylene to polyethylene [20].

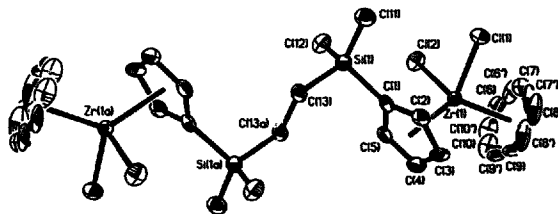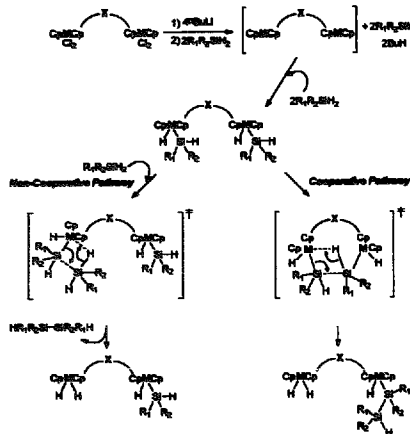In the present study, the monometallic complexes Cp$_2$TiCl$_2$ and Cp$_2$ZrCl$_2$ and the bimetallic complexes

Fig. 4. Projection view of [μ-(Me$_2$SiCH$_2$CH$_2$SiMe$_2$)(C$_5$H$_4$)$_2$][CpZrCl$_2$]$_2$ with thermal ellipsoids drawn at 50% probability and showing disorder in Cp groups.

Scheme 2. Proposed mechanism for the dehydrocoupling of $R_1R_2SiH_2$ using bimetallic Group 4 catalysts.

1–7 were compared as dehydrocoupling catalysts for $PhSiH_3$ in the presence of [n]BuLi. All of the reactions were carried out at room temperature with an Si/M/[n]BuLi ratio of 100/1/2.2, and the resulting polyphenylsilane was characterized by various physical methods. Aliquots of the reaction mixtures from dehydrocoupling reactions with Cp_2TiCl_2, Cp_2ZrCl_2 and complexes 1–6 were taken after 24 and 48 h of reaction time, and are defined as polysilane samples A–P in Table 4. The average molecular weight M_w, number average molecular weight M_n and polydispersity Pd of the polysilane for each of these samples were measured by GPC analysis, and are presented in Table 4. After 48 h of reaction time, the catalysts were quenched and the volatiles (including any unreacted $PhSiH_3$) were removed under vacuum. The percent mass recovery for each reaction is also listed in Table 4.

Fig. 5 shows the GPC traces for the polysilane derived from the titanium catalysts Cp_2TiCl_2, 1, 3 and 4 and trans-6 after 48 h of reaction time, designated as samples B, F, J, L and P. Fig. 6 shows the GPC traces derived from the zirconium catalysts Cp_2ZrCl_2, 2 and 5 after 48 h of reaction time, corresponding to samples D, H and N. The GPC traces shown in Figs. 5 and 6 are bimodal as a result of the presence of both linear and cyclic polyphenylsilane. It is generally understood that the lower molecular weight fraction (higher retention time) corresponds to the cyclic products, while the higher molecular weight fraction (shorter retention time) corresponds to the linear products [9,14]. The linear and

Table 4
Analysis of polyphenylsilane samples

Sample	Catalyst	Hours	M_w [a]	M_n [b]	Pd [c]	L/C [d]	Mass rec. (%)
A	Cp_2TiCl_2	24	1020	720	1.4	2.0	—
B	Cp_2TiCl_2	48	1480	900	1.6	2.2	90
C	Cp_2ZrCl_2	24	1620	1180	1.5	1.8	—
D	Cp_2ZrCl_2	48	1740	1140	1.5	2.5	92
E	1	24	1230	810	1.5	1.9	—
F	1	48	1680	930	1.8	2.1	94
G	2	24	2440	1400	1.7	4.8	—
H	2	48	2940	1590	1.9	5.5	90
I	3	24	1570	920	1.7	2.0	—
J	3	48	1440	910	1.6	1.7	94
K	4	24	1940	950	2.0	2.1	—
L	4	48	2010	940	2.1	2.2	93
M	5	24	2050	1210	1.7	2.7	—
N	5	48	1990	1230	1.6	3.5	88
O	trans-6	24	1510	950	1.6	2.5	—
P	trans-6	48	1590	960	1.7	2.1	85
Q [e]	—	—	570	550	1.0	—	—

		$PhBuSiH_2$		$H(PhSiH)_2H$	$H(PhSiH)_3H$	$H(PhSiH)_4H$	Mass rec. (%)
R [f]	trans-7	12		64	21	5	46
S [f]	cis-7	9		53	29	9	52

[a] Weight average molecular weight, determined by GPC.
[b] Number average molecular weight, determined by GPC.
[c] Polydispersity = M_w/M_n.
[d] Linear/cyclic ratio, determined by GPC integration.
[e] Cyclic component only, obtained from a mixture of polysilane products from condensation reactions with Cp_2TiCl_2, 1, 3, 4 and 6.
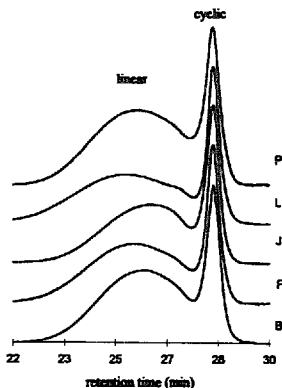[f] Percent of each oligomer, determined by GC/MS after 48 h of reaction.

Fig. 5. GPC traces for polyphenylsilane samples for samples B, F, J, L and P, derived from titanium catalysts listed in Table 4.

cyclic regions are labeled in the GPC trace for sample P (Fig. 5). The approximate ratios of linear/cyclic (L/C) products for samples A–P were determined from the integration of the two regions of the GPC trace, and are also listed in Table 4.

The ^{1}H NMR spectra were collected for the polysilane samples obtained from reactions with Cp_2TiCl_2, Cp_2ZrCl_2 and complexes 1–6 after 48 h, and the SiH region for each sample is shown in Fig. 7. This region consists of two broad massifs, and it is generally believed that the region downfield of 4.8 ppm is due to cyclic products, while the region upfield of 4.8 ppm is due to linear products [9,14]. Each of these spectra also show a triplet centered at 4.5 ppm corresponding to
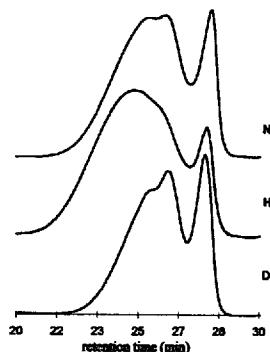
Fig. 6. GPC traces for polyphenylsilane samples for samples D, H and N, derived from zirconium catalysts listed in Table 4.
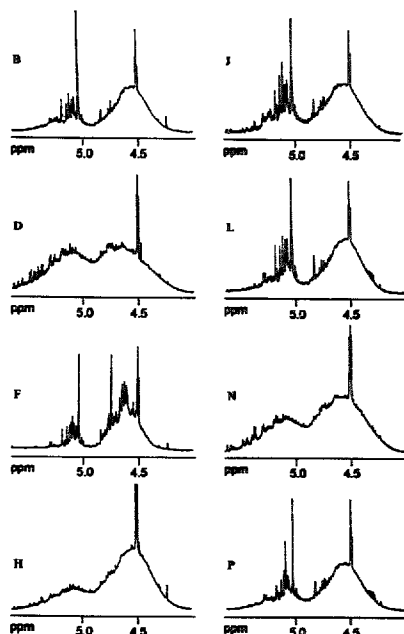
Fig. 7. ^{1}H NMR (500 MHz, C_6D_6) SiH regions for polyphenylsilane derived from the catalysts listed in Table 4 after 48 h of reaction time.

$PhBuSiH_2$, which is formed in the initial stages of the reaction of $PhSiH_3$, ^nBuLi and the metal complex [14].

One of the properties of the monobridged bimetallic catalysts which was examined in this study was the effect the length of the bridging unit X had on the dehydrocoupling reaction. Figs. 8 and 9 show the relationship between the number of atoms (#) in the bridge X and the measured M_w of the generated polysilane after 24 and 48 h of reaction for the titanium and zirconium systems respectively.

From Fig. 8 it can be seen that after 24 h of reaction, all of the bimetallic Ti catalysts produced polysilane with higher M_w values than did the monometallic system Cp_2TiCl_2. Also, the M_w increased as the number of atoms in the bridge X increased at the 24 h mark from 1020 for Cp_2TiCl_2 to 1940 for 4. However, this trend was lost after 48 h of reaction, when the M_w values for the polysilane produced from Cp_2TiCl_2 and complex 1 increased, while the M_w values for the polysilane produced from complexes 3 and 4 remained essentially unchanged. For the zirconium systems shown in Fig. 9, after 24 h of reaction both the bimetallic complexes 2 and 5 produced polysilane with higher M_w values than
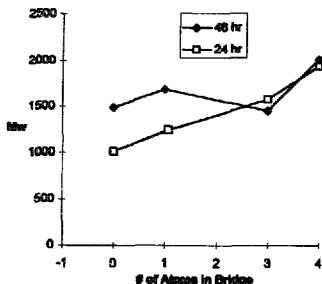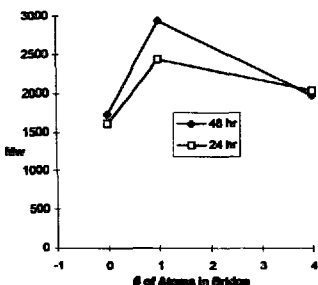
Fig. 8. M_w vs. the # of atoms in the bridging unit. Si/M = 100/1, M = Ti. For # of atoms in the bridge = 0, catalyst = Cp$_2$TiCl$_2$ (GPC runs A, B). For # of atoms in the bridge = 1, catalyst = 1 (GPC runs E, F). For # of atoms in the bridge = 3, catalyst = 3 (GPC runs I, J). For # of atoms in the bridge = 4, catalyst = 4 (GPC runs K, L).

did the monometallic Cp$_2$ZrCl$_2$. After 48 h of reaction time, the M_w for the polysilane generated from reactions with Cp$_2$ZrCl$_2$ and complex 5 remained at about 1700 and 2000 respectively. However, the M_w of the polysilane produced from complex 2 increased after 48 h from approximately 2500 to almost 3000.

As shown in Figs. 8 and 9, there does not seem to be a simple correlation between the length of X and the molecular weight of the polysilane produced. For the four titanium catalysts tested, the difference in reactivity was in the rate at which polysilane with M_w greater than 1000 was formed. The two bimetallic titanium complexes with longer bridges, 3 and 4, generated polysilane with higher M_w values early on in the reaction, but the M_w values did not increase after 24 h of reaction. The dehydrocoupling reactions with Cp$_2$TiCl$_2$ and 1 also formed polysilane with M_w values greater

Fig. 9. M_w vs. the # of atoms in the bridging unit. Si/M = 100/1, M = Zr. For # of atoms in the bridge = 0, catalyst = Cp$_2$ZrCl$_2$ (GPC runs C, D). For # of atoms in the bridge = 1, catalyst = 2 (GPC runs G, H). For # of atoms in the bridge = 4, catalyst = 5 (GPC runs M, N).

than 1000, but not until after 48 h of reaction. For the three zirconium systems tested, the best catalyst was the bimetallic complex 2, which has a one-atom bridge. This system produced polysilane with an M_w almost twice as high as that obtained from Cp$_2$ZrCl$_2$. The rates of formation of higher M_w polysilane also differed for the different zirconium catalysts. The M_w values of the polysilane generated from the monometallic Cp$_2$ZrCl$_2$ and the bimetallic complex 5 leveled off after 24 h, while the M_w of the polysilane derived from complex 2 continued to increase up to 48 h.

The dibridged titanium complexes trans-6 and the cis and trans isomers of 7 were also tested as dehydrocoupling catalysts for PhSiH$_3$. The GPC results for the polysilane produced from trans-6 after 24 and 48 h and are listed in Table 4 as samples O and P. The mass recovery for the polysilane produced from trans-6 was high (85%), and the M_w values after 24 and 48 h were between 1500 and 1600. However, the molecular weights of the polysilane generated from either trans-7 or cis-7 were too low to measure by GPC techniques. These lower molecular weight oligomers were characterized by GC/MS, and the percent of each oligomer after 48 h of reaction time is listed in Table 4 as samples R and S. Both the cis and trans isomers of 7 produced H(PhSiH)$_n$H with n = 2, 3 and 4, and both had mass recoveries of approximately 50%, indicating incomplete reaction of the starting PhSiH$_3$. The difference in the extent of dehydrocoupling for the dibridged trans-6 and the dibridged trans and cis-7 is most likely due to the steric differences in the Cp and Cp* ligands.

Several general features are evident from the dehydrocoupling results presented in Table 4 and Figs. 5-9. First, all of the dehydrocoupling reactions in which a zirconium catalyst was used produced polysilane of significantly higher M_w and M_n than did the corresponding titanium catalysts. This difference between titanium and zirconium systems in silane dehydrocoupling reactions is not unusual, and has previously been observed by our group [12,13] and by Harrod et al. [5]. The Pd was also similar for samples A-P (between 1.4 and 2.1). Another general feature of these dehydrocoupling reactions was a high mass recovery (except for trans and cis-7), which indicates essentially complete consumption of the starting PhSiH$_3$ after 48 h. Finally, all of the catalyst systems produced a mixture of both linear and cyclic products, although the L/C ratio was generally higher for the zirconium catalysts than for those of titanium.

The differences observed in the rates of PhSiH$_3$ dehydrocoupling and the M_w of the polysilane produced for the monometallic Cp$_2$MCl$_2$ and the bimetallic systems (Figs. 8 and 9) may be a result of a cooperative dehydrocoupling pathway, as proposed in Scheme 2. However, it is also possible that these differences in rates and M_w values for the bimetallic cata-

lysts are due to steric effects imposed by the bridges X. It has been suggested that substitution at one of the Cp rings of a Group 4 metallocene inhibits the formation of hydride bridged dimers, which are inactive in the dehydrocoupling reaction [8]. However, as Tilley has pointed out, too much steric bulk at the Cp rings hinders the dehydrocoupling reaction [8]. This is probably the reason the *trans* and *cis*-7 do not dehydrocouple $PhSiH_3$ past the oligomer stage.

As illustrated in Fig. 3, the *trans*-6 complex has the two metals which are locked on opposite sides of the molecule and the metals should not be able to interact in a cooperative manner, such as suggested in Scheme 2. The observation that the M_w values of the polysilane produced from *trans*-6 are very similar to those derived from Cp_2TiCl_2 and the monobridged bimetallic complexes 1, 3 and 4 suggests that a cooperative mechanism may not be a factor for any of these bimetallic systems. Furthermore, the fact that the *trans* and *cis* isomers of 7 produced approximately the same distribution of polysilane products supports a non-cooperative mechanism for dehydyrocoupling with bimetallic metallocene catalysts. However, this does not exclude the possibility of cooperative activity between the two metal centers in all of these bimetallic systems. It could be that both cooperative and uncooperative mechanisms are important in the dehydrocoupling reactions.

2.4. Isolation of all trans-[PhSiH]$_6$

From the GPC traces shown in Fig. 5, it can be seen that the dehydrocoupling of $PhSiH_3$ with any of the titanium catalysts produced a specific cyclic product with a retention time of 27.90 min. The GPC traces shown in Fig. 6 derived from the reactions in which a zirconium catalyst was used produced cyclic portions with slightly shorter and variable retention times. Furthermore, the ^1H NMR spectra presented in Fig. 7 for the polysilane produced from the titanium catalysts (samples B, F, J, L and P) show one prominent resonance in the cyclic region at 5.01 ppm. This cyclic component is absent from the ^1H NMR spectra for samples D, H and N, derived from the zirconium catalysts.

The cyclic product produced in the reactions with titanium was isolated by crystallization from a toluene solution of a polyphenylsilane sample produced from the combination of samples B, F, J, L and P. The FT-IR spectrum for these crystals showed a strong Si–H stretch at 2085 cm^{-1}, which has been previously attributed to all *trans*-(PhSiH)$_6$ [27], shown in Fig. 10. The GPC results from the crystals are presented as sample Q in Table 4. The GPC trace of the crystals showed one peak with a retention time of 27.90 min, and the SiH region of the ^1H NMR (C_6D_6) spectrum showed one singlet at 5.01 ppm. This cyclic product has also been observed by
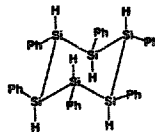

Fig. 10. Cyclic product from dehydrocoupling reactions with titanium catalysts, *trans*-(PhSiH)$_6$.

Harrod and co-workers from similar dehydrocoupling reactions of $PhSiH_3$ in which titanocene-based catalysts were used [27,28].

3. Summary

A series of monobridged bimetallic complexes of titanium and zirconium of the formula $[\mu$-$X(C_5H_4)_2]CpMCl_2]$ were prepared (complexes 1–5), and the synthesis and characterization of the new complexes 3, 4 and 5 were presented. The crystal structure of 5 was determined by X-ray diffraction. These bimetallic complexes were tested as catalysts for the dehydrocoupling of $PhSiH_3$, and found to produce mixtures of linear and cyclic polyphenylsilane, which were characterized by GPC analysis and ^1H NMR spectroscopy. After 48 h of reaction, the titanium catalysts all produced polysilane with M_w values between 1500 and 2000, while the zirconium systems produced polysilane with M_w values between 1700 and 2900. The dibridged *trans*-6 complex produced linear and cyclic polysilane with an M_w of 1600 after 48 h, and the dibridged *trans* and *cis*-7 produced low molecular weight oligomers. A cyclic product was isolated from the dehydrocoupling reactions in which a titanium catalyst was used, and was identified as the all *trans*-[PhSiH]$_6$ cyclic product.

4. Experimental

4.1. General considerations

All reactions unless otherwise noted were carried out under an atmosphere of N_2 using standard Schlenk techniques. The commercial compounds Cp_2TiCl_2 and Cp_2ZrCl_2 were purchased and used as supplied, and ^nBuLi was purchased in hexanes. The $PhSiH_3$ [29], $CpTiCl_3$ [30], $CpZrCl_3(THF)_2$ [31], $[\mu$-$(Me_2SiCH_2SiMe_2)(C_5H_5)_2]$ [21], $[\mu$-$(Me_2SiCH_2CH_2SiMe_2)(C_5H_5)_2]$ [22,23], 1 [18], 2 [16] and 6–8 [25] were prepared as previously described. Elemental analyses were performed by Atlantic Microanalytical Laboratories. ^1H and ^{13}C NMR data were recorded in $CDCl_3$ (referenced to $CHCl_3$) or C_6D_6

(referenced to C_6H_6) on a Bruker ARX500 equipped with either an inverse probe or a broad band probe. ^{29}Si NMR data were recorded on the Bruker in $CDCl_3$ (referenced externally to TMS) using INEPTRD (with a ^{1}H refocusing pulse, optimized for either $J = 7$ Hz for MeSi or $J = 100$ Hz for SiH). IR data were collected on a Mattson 6020 Galaxy Series FT-IR spectrometer (KBr). Mass spectral data (EI) were collected at 70 eV on a Hewlett-Packard model 5988A GC/MS instrument.

4.2. GPC analysis

GPC data were collected using a SSI 222D HPLC pump and Linear UV/Vis detector set at 260 nm, using three Waters Styragel columns (7.6 × 300 nm) in series (10^4Å, 10^3Å and 500 Å) with THF as the solvent (1.0 ml min^{-1}), and a Spectra Physics SP46000 Data Jet Integrator. The THF solvent was dried by distillation from CaH_2, filtered through a fine frit, and sonicated for 10 min before use. The average molecular weight M_w, number average molecular weights M_n and polydispersity Pd values of the polyphenylsilane samples were determined relative to ten polystyrene standards, which were purchased from Polysciences, Inc., with molecular weights in the range of 580 to 22000.

4.3. Synthesis of [μ-(Me₂SiCH₂SiMe₂)-(C₅H₄)₂][CpTiCl₂]₂ (3)

$Li_2[μ-(Me_2SiCH_2SiMe_2)(C_5H_4)_2]$ was obtained from the reaction of ^{n}BuLi (16.2 ml, 2.5 M) with [μ-(Me₂SiCH₂SiMe₂)(C₅H₅)₂] (2.11 g, 8.11 mmol) in hexanes (50 ml). The white solid was collected by filtration under N_2, washed with hexanes and dried in vacuo to provide a white powder (1.9 g, 86% yield). This dilithio salt (0.670 g, 2.46 mmol) was added to a Schlenk tube and dissolved in THF (20 ml). To this stirred solution, solid $(C_5H_5)TiCl_3$ (1.08 g, 4.82 mmol) was added to provide an intensely red reaction mixture, which gradually lightened in color to red-orange as orange microcrystals began to form on the sides of the Schlenk tube. The reaction mixture was stirred for 15 min, then allowed to stand at room temperature overnight. The crystals were then collected by filtration, washed with hexanes, and purified by Soxhlet extraction with CH_2Cl_2 to provide 0.85 g of 3 (55% yield, decomp. > 240 ºC). Compound 3 was found to contain 0.25 equiv. of CH_2Cl_2, which could not be removed by drying in vacuo or by washing with hexanes. Anal. Calcd for $C_{25}H_{32}Cl_4Si_2Ti_2(0.25CH_2Cl_2)$: C, 46.84; H, 5.06. Found: C, 46.49; H, 5.03. ^{1}H NMR (500 MHz, CDCl₃): δ 0.25 (s, 12H, SiMe₂), 0.42 (s, 2H, CH₂), 5.28 (s, 0.5H, CH₂Cl₂), 6.53 (s, 10H, C₅H₅), 6.58 (t, 2.4 Hz, 4H, C₅H₄), 6.81 (t, 2.3 Hz, 4H, C₅H₄). ^{13}C NMR (125 MHz, CDCl₃): δ 0.92 (SiMe₂), 3.59 (CH₂),

120.21 (C₅H₅), 120.56, 128.91, 133.99 (C₅H₄). ^{29}Si NMR (99 Hz, CDCl₃): δ −4.93 (SiMe₂).

4.4. Synthesis of [μ-(Me₂SiCH₂CH₂SiMe₂)-(C₅H₄)₂][CpTiCl₂]₂ (4)

Similarly, $Li_2[μ-(Me_2SiCH_2CH_2SiMe_2)(C_5H_4)_2]$ was obtained as a white powder (4.4 g, 88% yield) from the reaction of ^{n}BuLi (14.0 ml, 2.5 M) with [μ-(Me₂SiCH₂SiMe₂)(C₅H₅)₂] (4.79 g, 17.5 mmol) in hexanes (50 ml). This dilithio salt (1.00 g, 3.49 mmol) was allowed to react with $(C_5H_5)TiCl_3$ (1.53 g, 6.98 mmol) in THF (20 ml) in a manner identical to that described for 3. The orange-red microcrystals which formed were collected by filtration, washed with hexanes, and purified by Soxhlet extraction with CH_2Cl_2 to provide 1.1 g of 4 (50% yield, decomp. > 245 ºC). Compound 4 was also found to contain 0.25 equiv. of CH_2Cl_2, which could not be removed by drying in vacuo or by washing with hexanes. Anal. Calcd for $C_{26}H_{34}Cl_4Si_2Ti_2(0.25CH_2Cl_2)$: C, 47.66; H, 5.26. Found: C, 47.27; H, 5.21. ^{1}H NMR (500 MHz, CDCl₃): δ 0.25 (s, 12H, SiMe₂), 0.62 (s, 4H, CH₂CH₂), 5.28 (s, 0.5H, CH₂Cl₂), 6.52 (s, 10H, C₅H₅), 6.59 (t, 2.4 Hz, 4H, C₅H₄), 6.82 (t, 2.3 Hz, 4H, C₅H₄). ^{13}C NMR (125 MHz, CDCl₃): δ −2.61 (SiMe₂), 8.70 (CH₂CH₂), 120.14 (C₅H₅), 120.80, 129.20, 131.95 (C₅H₄). ^{29}Si NMR (99 Hz, CDCl₃): δ −2.26 (SiMe₂).

4.5. Synthesis of [μ-(Me₂SiCH₂CH₂SiMe₂)-(C₅H₄)₂][CpZrCl₂]₂ (5)

$Li_2[μ-(Me_2SiCH_2CH_2SiMe_2)(C_5H_4)_2]$ (0.703 g, 2.46 mmol) was added to a Schlenk tube and dissolved in THF (20 ml). To this stirred solution, $(C_5H_5)ZrCl_3(THF)_2$ (2.00 g, 4.92 mmol) suspended in a mixture of THF (10 ml) and hexanes (30 ml) was added dropwise. The reaction mixture developed a pale yellow/brown color, and a white precipitate began to form after 15 min. The mixture was stirred overnight at room temperature, the volatiles were then removed under vacuum and CH_2Cl_2 (20 ml) was added to precipitate the LiCl. The LiCl was removed by filtration under N_2 through a fine frit to provide a yellow filtrate which was concentrated (to 10 ml). Hexanes (20 ml) were added and the solution stored overnight at −50°C to afford small, white crystals, which were washed with hexanes to provide 0.85 g of 5 (48% yield, decomp. > 230 ºC). Anal. Calcd for $C_{26}H_{34}Cl_4Si_2Zr_2$: C, 42.96; H, 4.71. Found: C, 42.77; H, 4.77. ^{1}H NMR (500 MHz, CDCl₃): δ 0.26 (s, 12H, SiMe₂), 0.59 (s, 4H, CH₂CH₂), 6.43 (s, 10H, C₅H₅), 6.52 (t, 2.5 Hz, 4H, C₅H₄), 6.66 (t, 2.5 Hz, 4H, C₅H₄). ^{13}C NMR (125 MHz, CDCl₃): δ −2.71 (SiMe₂), 8.82 (CH₂CH₂), 115.94 (C₅H₅), 116.97, 125.46, 125.67 (C₅H₄). ^{29}Si NMR (99 Hz, CDCl₃): δ −3.21 (SiMe₂).

4.6. Crystallographic data collection and structure determination for [μ-(Me₂SiCH₂CH₂SiMe₂)-(C₅H₄)₂][CpZrCl₂]₂ (5)

Colorless prism-shaped crystals of **5** were obtained by slow recrystallization in a CH_2Cl_2 solution at room temperature. Data collection was performed using a Siemens SMART Charge Coupled Device (CCD) Detector system single crystal X-ray diffractometer using graphite monochromated Mo Kα radiation ($\lambda = 0.71073$ Å) equipped with a sealed tube X-ray source (50 kV x 40 mA) at −80°C. Preliminary unit cell constants were determined with a set of 60 narrow frames (0.3 in ω) scans. A total of 13 000 frames of intensity data were collected with a frame width of 0.3 in ω and counting time of 10 s/frame at a crystal to detector distance of 3.89 cm. The double pass method of scanning was used to exclude any noise. Data was collected at −80°C for a total time of 6.5 h. The collected frames were integrated using an orientation matrix determined from the narrow frame scans. SMART software package [32] was used for data collection and SAINT package [32] was used for frame integration. Analysis of the integrated data did not show any decay. Final cell constants were determined by a global refinement of *xyz* centroids of 3427 reflections. An absorption correction was applied to the data using equivalent reflections. The integration process yielded 9275 reflections of which 2898 ($2\theta < 52°$) were independent reflections.

Structure solution and refinement were carried out using the SHELXTL-PLUS (5.03) software package [32]. The structure was solved by direct methods and refined successfully in the space group $P2_1/n$. Full matrix least squares refinement was carried out by minimizing $\sum w(F_o^2 - F_c^2)^2$. The Cp carbons were disordered, and the rings were refined using partial occupancy, to a factor of 53% [C(6)–C(10)] and 47% [C(6')–C(10')]. The non-hydrogen atoms were refined anisotropically to convergence. All the hydrogen atoms were treated using appropriate riding models (AFIX m3). A projection view of the molecule with non-hydrogen atoms represented by 50% probability ellipsoids, and showing the atom labeling is presented in Fig. 4. Complete lists of bond distances, bond angles and positional and isotropic displacement coefficients for the hydrogen and non-hydrogen atoms are available from the authors and will be deposited with the Cambridge Structural Database. Additionally, a packing diagram is available from the authors.

4.7. Condensation reactions of PhSiH₃

General: all of the condensation reactions of $PhSiH_3$ were conducted following the same procedure, on a scale of 0.500 g $PhSiH_3$, with a ratio of Si/M of 100/1, and an M/*BuLi ratio of 1/2.2, under a blanket of N_2 in Schlenk tubes which were shielded from direct sunlight by aluminum foil. In a typical condensation reaction, an aliquot of *BuLi (2.5 M) was added to a stirred slurry of the monometallic or bimetallic complex in $PhSiH_3$.

The condensation reactions in which Cp_2TiCl_2, **1**, **3**, **4** or **6** were used proceeded with the formation of dark green reaction mixtures, which bubbled vigorously for approximately 1 min, then bubbled slowly for several hours. These mixtures generally thickened and became unstirrable within 24 h. When either the *cis* or *trans* isomers of **7** were used, the condensation proceeded with the formation of dark blue mixtures, which bubbled slowly for 24 h and remained stirrable after 48 h. The condensation reactions in which Cp_2ZrCl_2, **2** or **5** were used proceeded with the formation of yellow or orange reaction mixtures, which bubbled vigorously for approximately 5 min, then bubbled slowly for several hours. The mixtures for these reactions generally thickened and became unstirrable after 30 min. After the appropriate length of time, an aliquot was removed and dissolved in THF for GPC analysis. After 48 h of reaction, toluene was added and air was bubbled through the solution to quench the catalyst. The volatiles were removed under vacuum, the gummy to brittle residue was weighed and the percent mass recoveries are reported in Table 4.

4.8. Isolation of trans-[PhSiH]₆

The polyphenylsilane products obtained from dehydrocoupling reactions of $PhSiH_3$ using Cp_2TiCl_2, **1**, **3**, **4** and *trans*-**6** as catalysts (48 h of reaction time) were combined, dissolved in toluene and stored at 0°C for 7 days, resulting in the formation of white crystals. The crystals were isolated by decanting, washed with cold hexanes three times and finally dried under vacuum. GPC analysis of the crystals are tabulated in Table 4 as run Q. The spectral data were identical to that previously reported [25]. ^1H NMR (500 MHz, $CDCl_3$): δ 4.60 (s, 6H, SiH), 7.10 (m, 12H, C_6H_5), 7.25 (m, 6H, C_6H_5), 7.45 (m, 12H, C_6H_5). ^1H NMR (500 MHz, C_6D_6): δ 5.01 (s, 6H, SiH), 6.94 (m, 18H, C_6H_5), 7.54 (m, 12H, C_6H_5). ^{29}Si NMR (99 Hz, $CDCl_3$): δ −62.04. FT-IR (KBr): 2085 cm^{-1} (Si–H).

References

[1] R.D. Miller and J. Michl, *Chem. Rev.*, 89 (1989) 389.

[2] R. West, *J. Organomet. Chem.*, 300 (1986) 327.

[3] C.T. Aitken, J.F. Harrod and E. Samuel, *J. Organomet. Chem.*, 279 (1985) C11.

[4] (a) C. Aitken, J.F. Harrod and E. Samuel, *Can. J. Chem.*, 64 (1986) 1677. (b) C.T. Aitken, J.F. Harrod and U.S. Gill, *Can. J. Chem.*, 65 (1987) 1804. (c) J.F. Harrod, in M. Zeldin, K.J. Wynne and H.R. Allcock (eds.), *Inorganic and Organometallic Polymers: ACS Symposium Series 360*, American Chemical Society, Washington, DC, 1988, Chapter 7, p. 89. (d) J.F. Harrod, in K.G. Smith and E.C. Sanford (eds), *Progress in Catalysis*, Elsevier, Amsterdam, 1992, p. 147. (e) C. Aitken, J.P. Barry, F. Gauvin, J.F. Harrod, A. Malek and D. Rousseau, *Organometallics*, 8 (1992) 1732.

[5] J.F. Harrod, Y. Mu and E. Samuel, *Polyhedron, 10* (1991) 1239.

[6] V.K. Dioumaev and J.F. Harrod, *Organometallics, 13* (1994) 1548.

[7] (a) J.F. Walzer, H.G. Woo and T.D. Tilley, *Polym. Prepr., 32* (1991) 441. (b) T.D. Tilley and H.G. Woo, in J.F. Harrod and R.M. Laine (eds.), *Inorganic and Organometallic Oligomers and Polymers*, Kluwer, Netherlands, 1991, p. 3. (c) T.D. Tilly, N.S. Radu F.F. Walzer and H.G. Woo, *Polym. Prepr., 33* (1992) 1237. (d) H.G. Woo, J.F. Walzer and T.D. Tilley, *J. Am. Chem. Soc., 114* (1992) 7047. (e) T. Imori, R.H. Heyn, T.D. Tilley and A.L. Rheingold, *J. Organomet. Chem., 493* (1995) 83.

[8] T.D. Tilley, *Acc. Chem. Res.*, 26 (1993) 22.

[9] T.D. Tilley and T. Imori, *Polyhedron, 13* (1994) 2231.

[10] T. Nakano, H. Nakamura and Y. Nagai, *Chem. Lett., 86* (1989) 83.

[11] (a) J.Y. Corey, X.H. Zhu, T.C. Bedard and L.D. Lange, *Organometallics, 10* (1991) 924. (b) J.Y. Corey, J.L. Huhmann and X.H. Zhu, *Organometallics, 12* (1993) 1121. (c) R.M. Shaltout and J.Y. Corey, *Organometallics*, in press.

[12] J.Y. Corey and X.H. Zhu, *J. Organomet. Chem., 439* (1992) 1.

[13] J.Y. Corey, and X.H. Zhu, *Organometallics, 11* (1992) 672.

[14] R.M. Shaltout and J.Y. Corey, *Tetrahedron, 51* (1995) 4309.

[15] (a) Y.L. Hsiao and R.M. Waymouth, *J. Am. Chem. Soc., 116* (1994) 9779. (b) J P. Banovetz, H. Suzuki and R.M. Waymouth, *Organometallics, 12* (1993) 4700. (c) W. Uhlig, *J. Organomet. Chem., 402* (1991) C45. (d) J.Y. Corey, D.M. Kraichely, J.L. Huhmann, J. Braddock-Wilking and A. Lindeberg, *Organometallics, 14* (1995) 2704. (e) J.Y. Corey, D.M. Kraichely, J.L. Huhmann and J. Braddock-Wilking, *Organometallics, 13* (1994) 3408.

[16] K.P. Reddy and J.L. Petersen, *Organometallics, 8* (1989) 2107.

[17] (a) J.F. Buzinkai and R.R. Schrock, *Inorg. Chem., 28* (1989) 2837. (b) U. Siemeling, P. Jutzi, B. Neumann, H.G. Stammler and M.B. Hursthouse, *Organometallics, 11* (1992) 1328. (c) J.M. Manriquez, M.D. Ward, W.M. Reiff, J.C. Calabrese, N.L. Jones, P.J. Carroll, E.E. Bunel and J.S. Miller, *J. Am. Chem. Soc., 117* (1995) 6182.

[18] I.E. Nifant'ev, M.V. Borzov, A.V. Churakov, S.G. Mkoyan and L.O. Atovmyan, *Organometallics, 11* (1992) 3942.

[19] S. Jüngling and R. Mülhaupt, *J. Organomet. Chem., 460* (1993) 191.

[20] H. Lang, S. Blau, A. Muth, K. Weiss and U. Neugebauer, *J. Organomet. Chem., 490* (1995) C32.

[21] M. Kumada, H. Tsunemi and S. Iwasaki, *J. Organomet. Chem., 10* (1967) 111.

[22] D. Seyferth and H. Lang, *Organometallics, 10* (1991) 347.

[23] T. Ushioda, M.L.H. Green, J. Haggitt and X. Yan, *J. Organomet. Chem., 518* (1996) 155.

[24] (a) X.Z. Zhou, Y. Wang and S.S. Xu, *Chem. Res. Chin. Univ., 8* (1992) 239. (b) P. Jutzi, R. Krallmann, G. Wolf, B. Neumann and H.G. Stammler, *Chem. Ber., 124* (1991) 2391.

[25] J.Y. Corey, J.L. Huhmann and N.P. Rath, *Inorg. Chem., 34* (1995) 3203.

[26] T. Cuenca, A. Padilla, P. Royo, M. Parra-Hake, M.A. Pellinghelli and A. Tiripicchio, *Organometallics, 14* (1995) 848.

[27] H. Li, I.S. Butler and J.F. Harrod, *Appl. Spectrosc., 47* (1993) 1571.

[28] J.F. Harrod, H.-G. Woo and R. Shu, presented at the *29th Organosilicon Symp., Evanston, IL, March, 1996*, Abstr. A-12.

[29] A.E. Finholt, A.C. Bond, Jr., K.E. Wilzback and H.I. Schlesinger, *J. Am. Chem. Soc., 69* (1947) 2692.

[30] R.D. Gorsich, *J. Am. Chem. Soc., 82* (1960) 4211.

[31] G. Erker, K. Berg, L. Treschanke and K. Engle, *Inorg. Chem., 21* (1982) 1277.

[32] G.M. Sheldrick, Siemens Analytical X-ray Division, Madison, WI, 1995.